

## A NUMERICAL ANALYSIS OF A NEWLY DESIGNED ALL-TERRAIN ELECTRIC SCOOTER FRAME UNDER VARIOUS LOAD CONDITIONS

TSVETAN ILIEV\*

*St. Ap. and Gospeller Matthew Institute of Robotics, Bulgarian Academy of  
Science, Bulgaria*

[Received: 24 February 2025. Accepted: 15 June 2025]

doi: <https://doi.org/10.55787/jtams.25.55.2.250>

**ABSTRACT:** This study employs finite element analysis (FEA) to evaluate a novel all-terrain electric scooter frame, the Vinghen Ti1, under four loading conditions aligned with bicycle frame standards. Motivated by safety concerns in dynamic, varied terrains, the analysis adapts ISO 4210-6:2023 guidelines to simulate steady motion with potholes, a vertical drop, horizontal loading on the head tube, and rear wheel braking. A 3D FEA model with 63,734 tetrahedral elements and 124,544 nodes predicted stress distributions, revealing critical concentrations around welded joints, especially at the head tube and L-beams, with peak von Mises stresses up to 460 MPa. The study suggests design enhancements and underscores the importance of robust computational and experimental methods for advancing personal mobility safety and ensuring long-term durability.

**KEY WORDS:** FEA, scooter, frame, numerical analysis, electric scooter.

### 1 INTRODUCTION

The bicycle frame serves as the primary structural component of a bicycle, responsible for supporting both the rider and the mechanical elements [1]. Its design significantly influences the overall performance, durability, and safety of the bicycle [1]. Early investigations into the stresses experienced by bicycle frames involved experimental methods, such as strain gauge measurements, to assess the structural integrity under various loading conditions [2]. These foundational studies provided valuable insights but were often limited by the experimental techniques available at the time [2].

The advent of Finite Element Analysis (FEA) revolutionized the design and testing of bicycle frames [3]. FEA allows for comprehensive simulations of complex

---

\*Corresponding author e-mail: [tsvetan.iliev@vinghen.com](mailto:tsvetan.iliev@vinghen.com)

loading scenarios, enabling engineers to predict stress distributions, deformation patterns, and potential failure points without the need for extensive physical prototyping [3, 4]. This computational approach facilitates the optimization of frame geometry and material selection, leading to enhanced performance and safety [5]. Studies utilizing FEA have examined various aspects of bicycle frame design, including material comparisons and structural analyses under different loading conditions [5].

Typical dynamic situations encountered by bicycle frames include steady-state pedalling, vertical and horizontal impacts, and braking forces [6]. Understanding the frame's response to these dynamic loads is crucial for ensuring structural integrity and rider safety [6]. FEA has been instrumental in analysing these scenarios, providing detailed insights into the frame's behaviour under real-world conditions [6]. For instance, parametric finite element analyses have been conducted to assess the impact of different frame geometries on performance, aiding in the development of optimized designs [6].

In recent years, electric scooters have gained significant popularity as personal mobility devices, particularly in urban environments [7]. However, concerns regarding their safety have emerged, primarily due to design limitations that may not adequately address the dynamic loads encountered during operation [7]. To address these issues, a novel concept for an all-terrain electric scooter frame, named Vinghen Ti1, has been developed – international design registration number DM/239175. This design aims to enhance safety and performance across various terrains by incorporating robust structural features. Finite Element Analysis will be employed to evaluate the frame's response to typical stresses experienced by bicycle frames, ensuring its suitability for diverse operating conditions.

By leveraging advanced computational methods, this study seeks to contribute to the development of safer and more reliable electric scooter designs, addressing the growing demand for efficient and secure personal transportation solutions.

## 2 METHODS

This study analysed the stresses and deformations that occur on the Vinghen Ti1 electric scooter frame under four different loading conditions. The structural and testing requirements for bicycle frames are well defined in ISO 4210-6:2023 and include frame impact test, horizontal fatigue test, vertical fatigue test, dynamic strength test, rear triangle fatigue test, combined frame and fork test, and static strength test [8]. The requirements for electric scooter frames are more vaguely defined. As a result, four loading conditions were identified as most suitable for initial analysis of the novel frame and potential design optimisations and material selection:

- **Loading condition 1 (LC1) - steady state motion in straight line with pot holes.** This condition assumes that a person with a load of 700 N (71.4 kg)

is standing on the deck and riding the scooter with steady state in straight line and is subjected to peak vertical acceleration of 2G due to terrain/pot holes.

- **Loading condition 2 (LC2) - vertical loading.** The vertical loading scenario is modelled to represent a situation in which the scooter and the rider are dropped from a height of 0.3 m, representing riding off jumps and also covering for the lower level of stresses exerted by the frame from severe vibrations and potholes. It assumes 0.025m stopping distance, due to the deformation of the tyres. It also assumes equal weight distribution between the front and the rear hubs and simultaneous contact between both tyres and the ground. The peak load at this scenario is 8400N.
- **Loading condition 3 (LC3) - horizontal loading.** A 600N load is applied horizontally at the head-tube with the rear drop-outs being fixed.
- **Loading condition 4 (LC4) - rear wheel braking.** In this scenario, it is assumed that a hindrance is applied to the wheels, causing all forces to be concentrated on the rear wheel. A load of 200 N is applied to the rear dropouts, representing the effect of braking

All four cases assume a rigid body for the rider and rider's equal weight distribution over the complete area of the deck's supporting beams in LC1 and LC2.



Fig. 1. Tested frame with mesh.

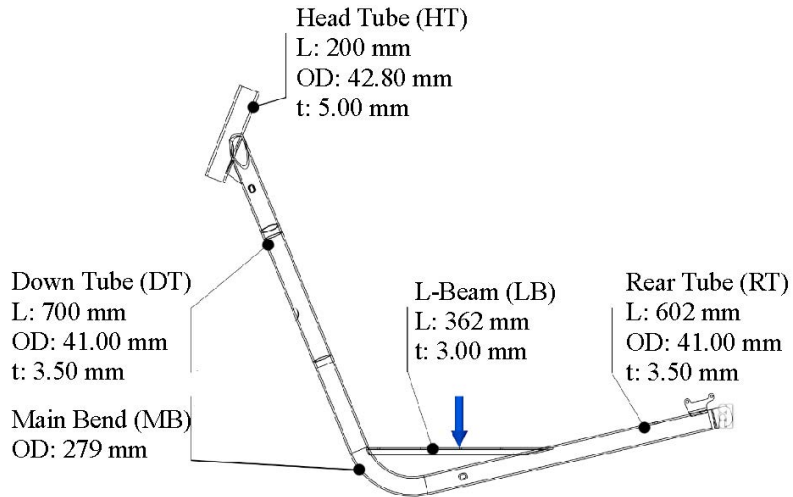


Fig. 2. Frame geometry.

A 3D finite element model was constructed with a parabolic mesh constructed of 63 734 solid tetrahedral elements with 124 544 nodes (Fig. 1).

The study was completed using Autodesk Fusion 360 2.0.21487 x86\_64 running on Windows 11 Pro 24H2 (26100.3194) on a PC with CPU Intel i7-12700H and GPU NVIDIA GeForce RTH 4060.

Figure 2 illustrates details and geometry of the frame and its tubes, including centre-to-centre tube lengths, angles, outside diameters, wall thicknesses. Fig. 3 illustrates the zones of interest that were used for the analysis in this study.

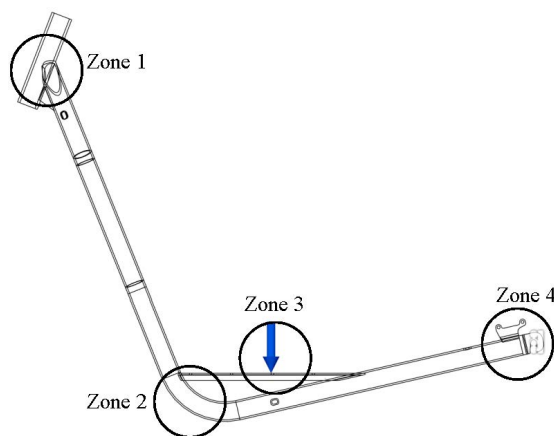


Fig. 3. Zones of interest in current study.

Boundary conditions in the form of loads and restraints were applied to the frame. Frictionless constraints were applied to the front and rear dropouts. Uniform, vertical loads were applied to the deck in loading conditions 1 and 2, and to the fork dropouts and to the rear dropouts respectively in loading conditions 3 and 4.

The material used for the frame in this analysis was Aluminium 6061 with specifications shown in Table 1.

Table 1. Material properties of aluminium 6061

Properties	Metric	Unit
Young's Modulus	68.90	GPa
Poisson's ratio	0.33	
Yield strength	275.00	MPa
Ultimate tensile strength	310.00	MPa

### 3 RESULTS

The regions of highest stress on the scooter's frame are presented in Table 2 for Load Case 1, Table 3 for Load Case 2, Table 4 for Load Case 3, and Table 5 for Load Case 4.

Table 2. Results Load Case 1

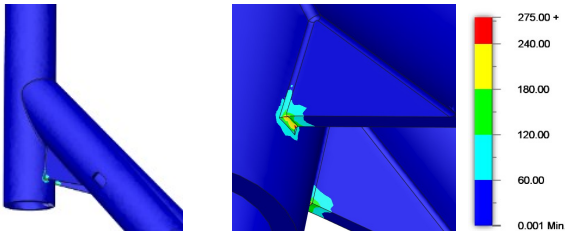
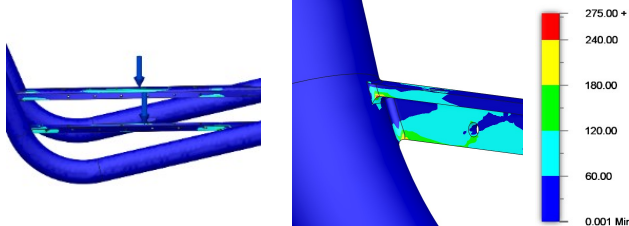
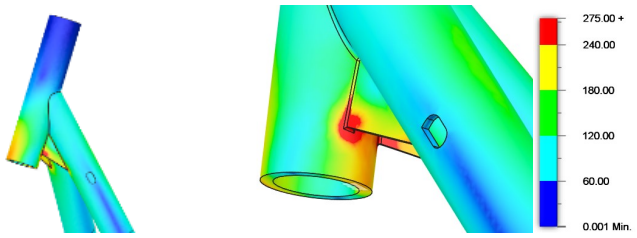
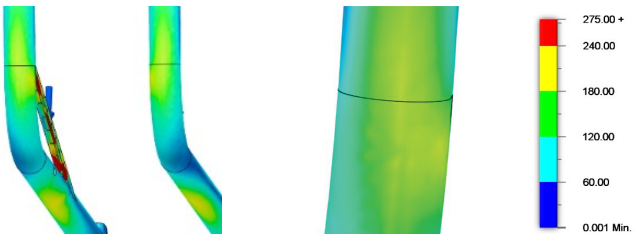
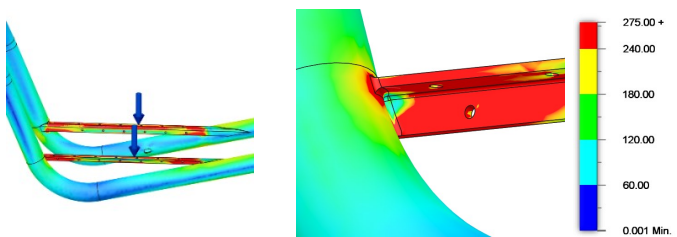
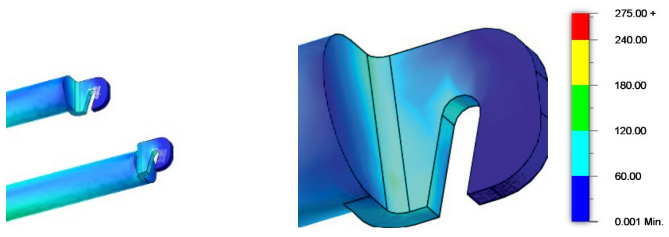
Load Case & Zone	Additional details	Von Mises stress
LC1 Zone 1		254 MPa
LC1 Zone 2		287 MPa

Table 3. Results Load Case 2

Load Case & Zone	Additional details	Von Mises stress
LC2 Zone 1		370 MPa
LC2 Zone 2		170 MPa
LC2 Zone 3		460 MPa
LC2 Zone 4		70 MPa

Under Load Case 1, Zone 1 experienced a peak von Mises stress of 254 MPa, which was observed in the welded joint area between the head tube and the strengthening ribs connecting it to the down tube. In Zone 2, the peak von Mises stress reached 287 MPa, located in the welded joint area between the L-beam and the main beam. Compared to Zone 1, Zone 2 exhibited higher average stresses, indicating a more distributed stress pattern in this region.

Table 4. Results Load Case 3

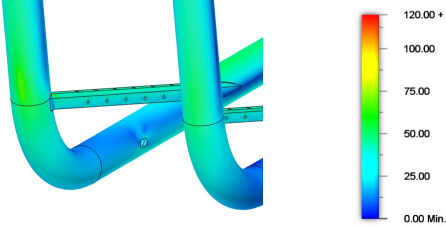
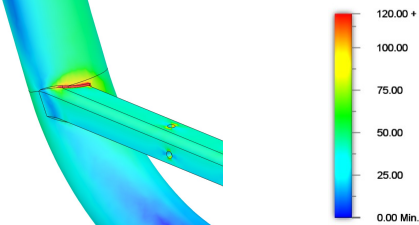
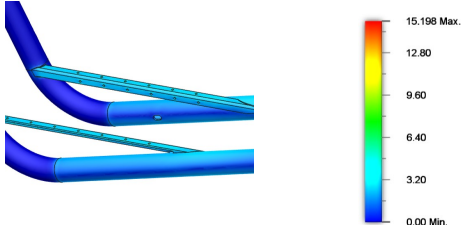
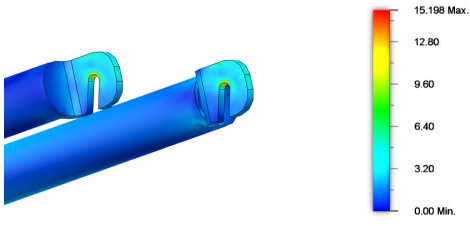
Load Case & Zone	Additional details	Von Mises stress
LC2 Zone 2		60 MPa
LC2 Zone 3		160 MPa

Table 5. Results Load Case 4

Load Case & Zone	Additional details	Von Mises stress
LC2 Zone 3		9 MPa
LC2 Zone 4		15 MPa

For Load Case 2, Zone 1 showed a peak von Mises stress of 370 MPa concentrated in the lower portion of the welded joint area between the head tube and the strengthening ribs. The stresses also extended into the head tube and the strengthen-

ing rib itself, although the peak concentration remained within the weld area. In Zone 2, peak stresses of 170 MPa were observed without any distinct concentration points. The highest stresses were recorded in Zone 3, with peaks reaching 460 MPa in the welded joint area and along the L-beam. Zone 4 displayed moderate stress levels, with peak stresses of 70 MPa observed around the 90-degree bend of the dropouts.

Load Case 3 resulted in moderate stress levels, with Zone 2 experiencing a peak von Mises stress of 60 MPa in the welded joint area between the L-beam and the main beam. In Zone 3, the peak stress reached 160 MPa, also concentrated in the welded joint area between the L-beam and the main beam.

In Load Case 4, stress levels were relatively low, with Zone 3 showing a maximum von Mises stress of 9 MPa distributed along the L-beams, while Zone 4 exhibited a peak stress of 15 MPa around the dropouts.

#### 4 DISCUSSION

The objective of this study was to employ FEA to perform an initial analysis of the strength of the proposed novel scooter frame using aluminium 6061 and main tubes with a wall thickness of  $t = 3.50$  mm.

Given the well-defined structural and testing requirements for bicycle frames outlined in ISO 4210-6:2023, and the lack of equivalent standards for scooter frames, the analysis partially adapted the bicycle frame requirements while incorporating deviations to account for differences in loading scenarios, such as the absence of a saddle and pedalling forces.

The FEA results indicate that under the tested load cases, the highest stress levels on the frame occur in Zone 1 and Zone 3. In Zone 1, the highest stress concentration is located at the welded joint area between the head tube and the strengthening ribs connecting it to the down tube. In Load Case 2, the peak von Mises stress in this zone was 370 MPa, concentrated in the lower area of the strengthening rib. Although the peak stress is localized in a small area, the surrounding zones, including the ribs and head tube, experience lower but significant stress levels. Zone 3 exhibited the highest overall stress concentrations, with peak von Mises stresses reaching 460 MPa in the welded joint between the L-beam and the main beam. These stresses extended along the length of the L-beam under heavy vertical loading, suggesting a potential risk of buckling. Zone 2 displayed moderate stress levels, with a peak of 170 MPa, and Zone 4 exhibited lower stress levels, with a maximum of 70 MPa.

Von Mises stress, which is used to predict material yielding under complex loading, serves as an important parameter in assessing the frame's strength and identifying weaknesses. Aluminium 6061, with a yield strength of 275 MPa, undergoes plastic deformation when this threshold is exceeded, increasing the risk of fatigue and failure under cyclic loading. Load Case 1 resulted in stress levels below the yield strength in

most areas, except for localized points in Zone 3 where the L-beam meets the main beam. These stresses arise from the natural tendency of the frame to bend at the main joint under vertical loading, with the L-beams counteracting this tendency and consequently experiencing higher stress levels. The L-beams serve a dual role, providing stiffness to the frame and supporting both the electronics box housing the battery and controller and the deck where the rider stands.

In Load Case 2, which applies the highest vertical load, stress levels exceeded the yield strength in Zones 1 and 3. In Zone 1, risk mitigation measures could include introducing stress-dissipating features, such as chamfers or changes to the angle at which the ribs join the head tube. In Zone 3, stress levels suggest that the L-beams could buckle under heavy loading. This could be addressed by increasing the cross-sectional area of the L-beams, either by thickening the material or extending the profile length and increasing the radii of the L-beam bends to reduce stress concentration. Strengthening the welds at these points by increasing contact areas would further improve structural integrity.

Comparison with existing literature reveals parallels between the stress patterns observed in this study and those found in studies on traditional bicycle frames. Akhyar and Husaini observed peak stresses around the seat post in scenarios similar to Load Cases 1 and 3, while stresses around the dropouts were prominent in scenarios similar to Load Case 4 [9]. Covill and Allard also performed FEA on a diamond-shaped bicycle frame and found elevated stress levels around the welds between the head tube and the top and down tubes under loading conditions comparable to Load Case 1 [10]. These findings are similar to the peak stress concentrations observed in Zone 1 of the scooter frame analysed in this study, particularly around the head tube strengthening ribs. Covill and Allard also emphasized the importance of fatigue strength, citing 500 million cycles as a standard benchmark for aluminium bicycle frames [10]. Similarly, Syung Lan and Wang Zhang reported stress concentrations around the seat post under conditions akin to Load Case 1 in their analysis of a diamond-shaped frame [11]. Rontescu and Cicic conducted FEA on an aluminium 6061 diamond-shaped frame and reported stress concentrations around the seat post and head tube welds. Their frame design, weighing 6 kg, is notably heavier than the 4 kg of the scooter frame analysed here, demonstrating the scooter frame's superior weight-to-strength performance [12].

A key difference between this study and the literature lies in the location of peak stresses. For bicycle frames, the highest stress concentrations typically occur around the seat post due to the rider's weight being concentrated there. In contrast, for the scooter frame, the rider's weight is distributed further forward, closer to the head tube, resulting in peak stresses around Zone 1. This difference was anticipated due to the distinct design and usage of the two vehicle types.

The findings of this study demonstrate that a novel scooter frame, blending concepts from bicycles and scooters, can be designed to be safe, comfortable, and lightweight. The frame's ability to accommodate larger wheels — up to 28 inches in the front and 20 inches in the rear — enhances stability, comfort, and performance on varied terrains. At a weight of just 4 kg, the frame offers significant advantages over traditional e-bike frames, which typically weigh around and over 6 kg.

Despite these promising results, the study has limitations. The FEA assumed homogeneous material properties across the frame, including the welds, and did not account for weld-specific variations. The model treated the rider as a single, rigid body, neglecting dynamic load distribution. Additionally, the assumption of simultaneous ground contact of both wheels in Load Case 2 may not fully reflect real-world conditions. Most critically, this study focused on static loading, whereas fatigue and cyclic loading are vital for understanding long-term performance and safety.

Future work should address these limitations by incorporating the proposed design modifications and conducting additional FEA. Experimental validation is essential to ensure the reliability of the results. Fatigue analysis and dynamic simulations would provide a deeper understanding of the frame's performance and safety under real-world conditions. Nonetheless, this study establishes a solid foundation for identifying critical stress-prone areas and developing targeted solutions to improve the scooter frame's design. It highlights the potential of this innovative frame to deliver a safe and versatile mobility solution for diverse terrains and user needs.

## 5 CONCLUSIONS

The FEA results revealed that the most significant stress concentrations occurred in welded areas, particularly around the head tube (Zone 1) and L-beams (Zone 3), with peak von Mises stresses surpassing the yield strength of Aluminium 6061 in certain load scenarios. Although some stress concentrations were localized, their magnitudes underscore the potential for structural compromise under repeated or heavy loads. The comparison with existing research on bicycle frames shows that while patterns of high stress around welds are common, differences in weight distribution shift the location of peak stresses in scooter designs.

To mitigate these risks, targeted design changes, such as reinforcing weld geometry, modifying beam cross-sections, or incorporating stress-dissipating features, are recommended. Additionally, future studies should address fatigue and cyclic loading to capture the long-term performance of the frame, supplemented by experimental validation for reliability. Overall, this work demonstrates that a carefully engineered electric scooter frame can meet rigorous structural demands, offering a safer and more versatile mobility solution in diverse operating conditions.

## REFERENCES

- [1] P. SARATH, D. AKASH, H. HRISHIKESH, S.D. NIMISHA, JINUCHANDRAN (2021) Stress Analysis of Bicycle Frame using Different Materials by FEA. *GRD Journal for Engineering* **6** 14-20.
- [2] L. PETERSON, K. LONDRY (1986) Finite-Element Structural Analysis: A New Tool for Bicycle Frame Design The Strain Energy Design Method. *Bicycling Magazine's Newsletter for the Technical Enthusiast* **5**(2).
- [3] P.D. SODEN, M.A. MILLAR, B.A. ADEYEFA, Y.S. WONG (1986) Loads, stresses, and deflections in bicycle frames. *The Journal of Strain Analysis for Engineering Design*. **21** 185-195.
- [4] C. LIN, S. HUANG, C. LIU (2017) Structural analysis and optimization of bicycle frame designs. *Advances in Mechanical Engineering*. **9**.
- [5] K. KADAM, N. SAMBHAR, N. BORA, S. BHAKARE, S. GAIKWAD (2020) Design and Analysis of E-Scooter Chassis Frame. *International Research Journal of Engineering and Technology*. **7** 7138-7146.
- [6] V. BULEJ *et al.* (2022) Analysis of symmetrical/asymmetrical loading influence of the full-suspension downhill bicycle's frame on the crack failure formation at a critical point during different driving scenarios and Design Improvement. *Symmetry* **14** 255.
- [7] B. SAVITSKY *et al.* (2021) Electric bikes and motorized scooters - popularity and burden of injury. Ten Years of National Trauma Registry experience. *Journal of Transport and Health* **22** 101235.
- [8] INTERNATIONAL ORGANIZATION FOR STANDARDIZATION (2023) Cycles — Safety requirements for bicycles.
- [9] A. AKHYAR, H. HUSAINI, I. HASANUDDIN, F. AHMAD (2019) Structural simulations of bicycle frame behaviour under various load conditions. *Materials Science Forum* **961** 137-147.
- [10] D. COVILL, P. ALLARD, J.-M. DROUET, N. EMERSON (2016) An assessment of bicycle frame behaviour under various load conditions using numerical simulations. *Procedia Engineering* **147** 665-670.
- [11] T. LAN, H. ZHANG, J. GAO, X. DAI (2020) Design and optimized simulation of bicycle frame structure. *2020 IEEE Eurasia Conference on IOT, Communication and Engineering (ECICE)* 301-304.
- [12] C. RONTESCU, T. CICIC, C. AMZA, O. CHIVU, D. DOBROTA (2015) Choosing the Optimum Material for Making a Bicycle Frame. *Metalurgija* **54** 679-682.